

# PosterO: Structuring Layout Trees to Enable Language Models in Generalized Content-Aware Layout Generation

HsiaoYuan Hsu and Yuxin Peng\*

Wangxuan Institute of Computer Technology, Peking University

kslh99@stu.pku.edu.cn, pengyuxin@pku.edu.cn

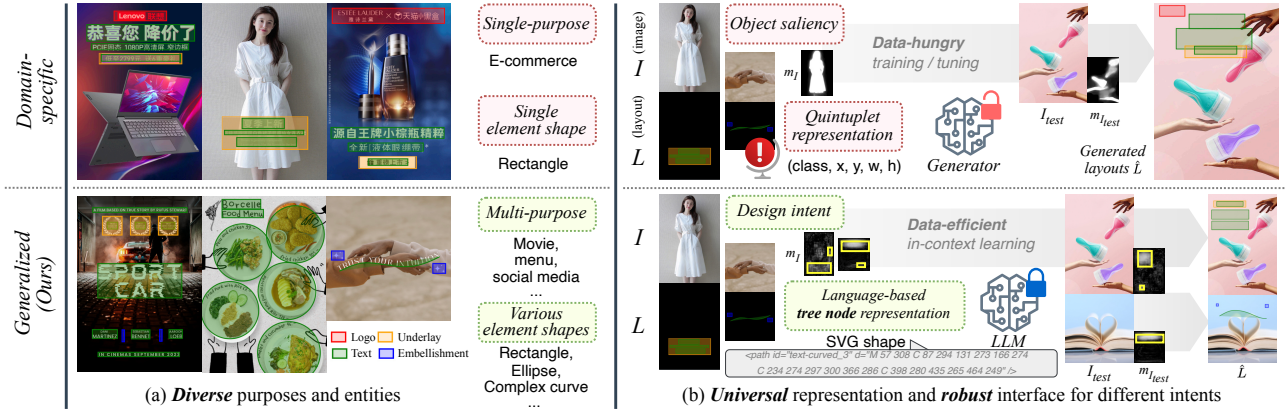


Figure 1. Illustration of the generalized settings in content-aware layout generation from both (a) data and (b) approach perspectives.

## Abstract

In poster design, content-aware layout generation is crucial for automatically arranging visual-textual elements on the given image. With limited training data, existing work focused on image-centric enhancement. However, this neglects the diversity of layouts and fails to cope with shape-variant elements or diverse design intents in **generalized** settings. To this end, we proposed a layout-centric approach that leverages layout knowledge implicit in large language models (LLMs) to create **posters** for **omnifarious** purposes, hence the name **PosterO**. Specifically, it structures layouts from datasets as trees in SVG language by **universal shape**, **design intent vectorization**, and **hierarchical node representation**. Then, it applies LLMs during inference to predict new layout trees by in-context learning with **intent-aligned example selection**. After layout trees are generated, we can seamlessly realize them into poster designs by editing the chat with LLMs. Extensive experimental results have demonstrated that PosterO can generate visually appealing layouts for given images, achieving new state-of-the-art performance across various benchmarks. To further explore PosterO’s abilities under the generalized settings, we built **PStylish7**, the first dataset with multi-purpose posters and various-shaped elements, further offering a challenging test for advanced research. Code and dataset are publicly available at <https://thekinsley.github.io/PosterO/>.

\*Corresponding author.

## 1. Introduction

Content-aware layout generation makes the poster design process intelligent by automatically arranging visual-textual elements on given images. As the demand for effective design grows rapidly, a mainstream platform surpasses 185 million monthly users [3], and 90% of survey participants take AI-empowered features as key considerations [2]. This technology is gaining more attention for its practical value in various applications [32, 49, 50, 53], as shown in Fig. 1.

Unlike other generation tasks [22, 43], collecting image-layout pairs for the target task requires costly annotation and inpainting processes [19, 55]. Therefore, existing work has incorporated object hints [4, 55], prior information [7, 19], retrieved references [17, 31], and augmented data [44] to confront the challenge of training data scarcity. However, because these are mainly image-centric enhancements without increasing the adaptability and diversity of layouts, they are prone to get trapped in the local solution space [18]. On the other hand, while leveraging related knowledge implicit in large language models (LLMs) [11, 37, 42, 47] showed the potential for layout-centric enhancements [12, 46], existing work [31, 44] has suffered from the semantically impoverished layout representations. The two primary issues are the monotonous rectangular shape of elements and the isolated visual constraints, which led to failures at capturing the complexity of real-world layouts and the intricate visual relationship between images and elements.

To pursue data efficiency and semantic richness required for advances in content-aware layout generation, we proposed **PosterO** to enable in-context learning (ICL) of LLMs by structuring *layout tree* representations. Specifically, it consists of *three* procedures, including (a) **layout tree construction** that jointly represents layout elements and design intents (*i.e.*, available areas on images) as hierarchical nodes in SVG trees [9], (b) **layout tree generation** that dynamically selects intent-aligned learning examples for the test input to facilitate ICL, and (c) **poster design realization** that integrates design materials into the generated layout trees to create posters in the subsequent chats with LLMs.

We conducted extensive experiments on public benchmarks [19, 55] and demonstrated that PosterO has achieved new *state-of-the-art* performance. It particularly shows stability in managing domain adaption problems [52] and spatial distribution shifts [17] that make the current approaches stumped. In additional efforts, we enhanced the evaluation process through newly added intent-aware content metrics that are more credible than currently used saliency-aware ones. We also demonstrated the adaptability of PosterO to different design intents and small-scale LLMs [35], highlighting its applicability. To further explore its potential under the **generalized** settings of diverse poster purposes (*e.g.*, commercial or education) and shape-variant elements (*e.g.*, circles or curves), we built the first dataset, **PStylish7**, consisting of 152 few-shot learning samples and 100 test images, covering *seven* representative poster purposes and *eight* element types. Serving as a challenging test, it is believed to facilitate advanced research in this field.

We summarize the contribution of this paper as follows:

- A language-based content-aware layout representation, **layout tree**, uses hierarchical nodes to model both layout elements and design intents with arbitrary shapes.
- A layout-centric approach, **PosterO**, leverages implicit knowledge of LLMs by applying a few intent-aligned layout trees as examples to perform in-context learning.
- Extensive evaluations and newly added metrics verify the superior effectiveness of PosterO in confronting various adaptation problems that plague current approaches.
- A dataset for generalized content-aware layout generation, **PStylish7**, incorporates seven representative poster purposes and eight shape-variant element types.

As our best knowledge, this work is the first to consider the generalized settings of content-aware layout generation.

## 2. Related Work

### 2.1. Content-aware Layout Generation

Apart from general layout tasks [1, 15, 23, 25, 28], content-aware layout generation is a cross-modal task [10, 16] integrating visual conditions, *i.e.*, image canvases, which are inherent in various real-world applications [32, 49, 50, 53],

highlighting its practical utility. With advances in deep generative models, data-centric approaches have become dominant in this field, categorized into GAN-based [18, 19, 52, 55], auto-regression-based [4, 5, 17, 30], and diffusion model-based [7, 27] approaches.

Entering into data construction of image-layout pairs, CGL-GAN [55] leveraged an inpainting model [45] to remove design elements from posters and a saliency object detection model [48] to give generative networks additional hints about image compositions. Similar saliency-enhanced paradigm [26, 39, 40] has been adopted by most subsequent approaches. Dealing with limited training data, DS-GAN [19] introduced prior knowledge [14, 29] to arrange layout elements in a meticulously designed order, making the patterns existing in the data more efficiently mined. RALF introduced retrieval augmentation, leveraging a composition-aware similarity evaluation model [13] to find the nearest neighbors for a given image, and incorporating their layout features [23] as additional inputs for the generative network. Moreover, Chai et al. [7] adapted a general layout diffusion model [6] for content-aware tasks by incorporating aesthetic constraints and a saliency-aware layout plausibility ranker.

As current approaches are engaged in image-centric enhancement yet seldom expand the diversity of layouts, the accessible solution space is narrowed, impeding their ability to address spatially varying design intents across different applications. In light of this, we propose a layout-centric, intent-aware approach in this work.

### 2.2. Language Model-based Layout Generation

While numerical layout representations risk losing the semantic information of attributes [46], current advances in large language models (LLMs) [11, 42, 47] open up new possibilities with HTML-based [31, 38], CSS-based [8, 12], and SVG-based [44, 46] language representations as these approaches enable leverage of layout knowledge implicit in LLMs. However, due to the challenge of guiding LLMs to perceive visual content, only a few approaches [31, 44] have supported content-aware layouts.

LayoutPrompter [31] represented each layout element as a `<div>` in HTML. While adopting a saliency paradigm, it only extracted the minimum bounding rectangle from the binary map as coarse content constraints and then retrieved layout examples for in-context learning. In contrast, PosterLlama [44] adopted a SVG-based representation [46] using `<rect>` shapes. It then fine-tuned DINOv2 [36, 56] with CodeLlama [20, 42] enhanced by data augmentation [54].

As current approaches employed monotype element representations and isolated visual representations, they failed to exploit the rich semantics of languages nor explicitly capture the relationship between elements and images. In light of this, we propose layout trees to represent various-shaped elements and visual hints jointly.

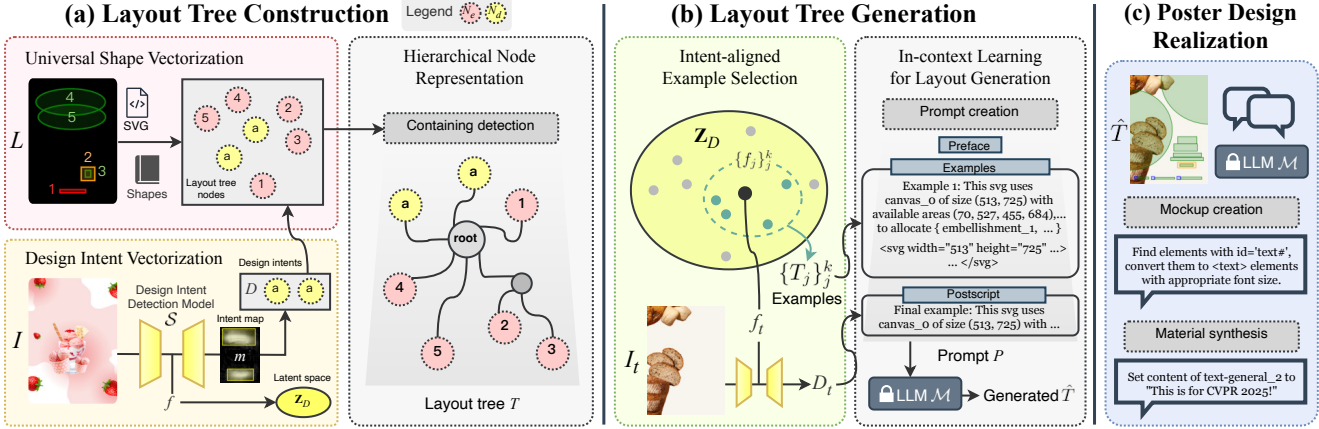


Figure 2. An overview of PosterO. First, (a) takes image-layout pairs  $(I, L)$  from datasets as input for data preparation, jointly modeling various-shaped elements  $E$  and design intents  $D$  towards layout trees  $T$  and building up the latent space of  $D$ . Then, (b) takes test images  $I_t$  as input and searches examples based on the predicted design intents  $f_t$  to apply LLM  $\mathcal{M}$  through in-context learning. After obtaining generated layout trees  $\hat{T}$ , (c) can continue the conversation with  $\mathcal{M}$  to create poster designs seamlessly.

### 3. The Proposed Approach: PosterO

Considering the limitations of image-centric and language model-based approaches, we propose PosterO. It is layout-centric and enables large language models (LLMs) to generate visually appealing layouts for given images by structurally representing the content-aware layouts as *trees*  $T$  in SVG language. An overview of PosterO is shown in Fig. 2. In brief, it is composed of *three* procedures, namely, (a) **layout tree construction** for data preparation, (b) **layout tree generation** applying an LLM  $\mathcal{M}$  through  $k$ -shot in-context learning, and (c) **poster design realization** through the subsequent chat with  $\mathcal{M}$ .

#### 3.1. Layout Tree Construction

##### 3.1.1. Universal Shape Vectorization

In content-aware layout generation, each data pair contains an image  $I$  and a layout  $L$ . Usually,  $L$  is represented as a set of numerical tuples  $\{e_i\}_i^n = \{(c_i, b_i)\}_i^n$ , where  $c_i$  and  $b_i = (x, y, w, h)$  indicate the category and bounding box of the  $i$ -th element  $e_i$  out of all  $n$  elements. As this is adequate only for rectangular elements, a more generalized representation becomes essential for the diverse shapes encountered in real-world posters, such as circles and curves. In light of this, SVG (Scalable Vector Graphics) emerges as an ideal choice because of its ability to represent arbitrary shapes and, more importantly, its nature as a language to facilitate the layout knowledge implicit in LLMs.

Following the published SVG standards [9], we define five shapes to encompass a wide range of elements typically found in posters, as shown in Fig. 3. First, (a) **regular rectangle** is vectorized using `<rect>`. Also, its two variants, including (b) **vertical rectangle** sensitive to the aspect ratio and (c) **rotated rectangle** using the `rotate` function in the `transform` attribute to indicate the rotation degree.



Figure 3. Various shapes of elements in PStylish7 dataset.

When delving into more intricate shapes, (d) **ellipse** is vectorized using `<ellipse>`, which can also handle the circle as a special case, and (e) **complex curve** is vectorized using `<path>` approximated by multiple cubic Bézier curves.

##### 3.1.2. Design Intent Vectorization

In addition to visual-textual elements, the design intents associated with the layout  $L$  must also be vectorized. Specifically, design intents  $D$  are embodied by a set of areas within the image  $I$ , suitable or intended for placing the elements. By incorporating these areas' representations  $N_D$ , the layout tree becomes content-aware and capable of conveying visual relationships between elements and images to LLMs, which cannot 'see' the images. As  $D$  can be learned from existing data or customized case by case, this also provides a flexible interface for indicating various purposes.

By leveraging image-layout pairs from posters with a similar purpose, a design intent detection model  $\mathcal{S}$  based on U-Net [41] is trained in a semi-supervised manner. Referring to [18],  $\mathcal{S}$  takes the bitmap of layout elements as the

supervision signal during the optimization, while the consistency loss is canceled to clearly segment out the areas. With the pre-trained  $\mathcal{S}$ , PosterO can obtain design intents  $D$  aligning the target purpose for any image  $I$ . Specifically, after thresholding and morphological operations, we approximate the contour of the predicted intent maps  $m$  and vectorize the obtained irregular areas using `< polygon >` in SVG language. An example is shown in Fig. 3(f). Besides, the intermediate embeddings  $f = \mathcal{S}_e(I)$ , where  $\mathcal{S}_e$  denotes the last block of the encoder, are also collected to serve as their representations in the latent space of design intents  $\mathbf{Z}_D$ .

### 3.1.3. Hierarchical Node Representation

As the nodes of layout elements  $N_E$  and design intents  $N_D$  are in place, the layout tree  $T$  is constructed and encapsulated within an SVG container aware of the image resolution  $(w_I, h_I)$ , as: `<svg width="{}w_I{}" height="{}h_I{}" xmlns="http://www.w3.org/2000/svg">{N_D}{N_E}</svg>`.  $N_D$  is put ahead to ensure that  $N_E$  is arranged considering their probabilistic dependencies in the autoregression, thus generating suitable content-aware layouts. In addition, as the special elements that wrap around others, such as underlays, are usually used in poster design, a novel hierarchical representation explicitly modeling these enveloping properties is proposed. Specifically,  $N_E$  is sorted by prioritizing underlays with larger areas. Then, given a node  $N_a$  and the corresponding nodes  $N_B = \{N_b \mid N_b \in \{N_E\}_{a+1}^n \wedge C(N_a, N_b)\}$ , where the condition function  $C(\cdot)$  is defined as:

$$\begin{aligned} C(\cdot) = & (|N_a.x - N_b.x| \leq \epsilon) \wedge (|N_a.y - N_b.y| \leq \epsilon) \\ & \wedge (|N_a.x + N_a.w - N_b.x - N_b.w| \leq \epsilon) \quad (1) \\ & \wedge (|N_a.y + N_a.h - N_b.y - N_b.h| \leq \epsilon), \end{aligned}$$

a subtree is constructed as `<svg x="{}N_a.x{}" y="{}N_a.y{}">{N'_a}{N'_B}</svg>` and inserted at the position of  $N_a$ , where the processed  $N'_i$  has the relative geometry attributes  $(N'_i.x, N'_i.y) = (N_i.x - N_a.x, N_i.y - N_a.y)$ . All leaf nodes of  $T$  are assigned unique identifiers  $id="{}c_{i-i}{}"$  to facilitate precise manipulation and querying.

## 3.2. Layout Tree Generation

### 3.2.1. Intent-aligned Example Selection

Upon findings from [34], LLMs are capable of in-context learning (ICL), requiring only a few examples to perform downstream tasks. This significantly reduces the need for task-specific data and avoids the extensive costs or catastrophic forgetting [24, 33] associated with fine-tuning. To make the best use of layout knowledge implicit in LLMs during ICL, selecting examples that align with the design intent is crucial. Therefore, given the test image  $I_t$ , its embedding  $f_t$  is first extracted by the detection model  $\mathcal{S}$ ; subsequently,  $k$  layout trees  $\{T_j\}_j^k$  are selected as in-context examples, where their embeddings  $\{f_j\}_j^k$  are the  $k$  closest to  $f_t$  in the latent space  $\mathbf{Z}_D$ .

### 3.2.2. In-context Learning for Layout Generation

To provide clear structure and objectives in the prompt  $P$  for the LLM  $\mathcal{M}$ , each intent-aligned example  $T_j$  is preceded by a short sentence that informs its number  $j$ , the resolution of its corresponding image, design intents  $D$ , and identifiers of its nodes, as shown in Fig. 2(b). The example field is then encapsulated within a preface and postscript, with the postscript delivering the request message of the test image  $I_t$  through a short sentence mirroring that of the example. Complete prompts  $P$  are presented in supplementary material. Finally, by inputting  $P$  into  $\mathcal{M}$  and interpreting the responses, PosterO completes the layout generation process.

## 3.3. Poster Design Realization

Benefiting from the essence of the generated layout tree  $\hat{T}$  as graphics and the rigid `id` assignment for elements, guiding  $\mathcal{M}$  to transform  $\hat{T}$  into a practical poster design is feasible and straightforward. Specifically, the transformation contains *mockup creation*, where shape elements are converted to `<text>` or `<image>` regarding their categories, and *material synthesis*, where elements are filled with actual design contents, *e.g.*, slogans and hyperlinks to images. Notably, this transformation is achieved with zero-shot learning, yet  $\mathcal{M}$  brings impressive results (in supplementary material) and even predicts suitable font sizes for texts, highlighting the value of design knowledge implicit in LLMs.

## 4. Experiments

### 4.1. Datasets

To evaluate the proposed PosterO, two public e-commerce poster datasets are used, while their train+valid/annotated test/unannotated test splits are allocated as in [17] to ensure a fair comparison with existing work. Specifically, **PKU PosterLayout** [19] comprises 8,734/1,000/905 images with three layout element types, including text, logo, and underlay; **CGL** [55] comprises 54,546/6,002/1,000 images with four layout element types, including text, logo, underlay, and embellishment. Furthermore, to explore PosterO’s abilities under the generalized settings, we built the first multi-purpose poster dataset, **PStylish7**, containing layout elements of various shapes. More details about PStylish7 are depicted in Sec. 4.6 and supplementary material.

### 4.2. Evaluation Metrics

Following previous work [17, 19, 55], we use graphic and content metrics. **Graphic metrics** include overlay  $Ove \downarrow$ , alignment  $Ali \downarrow$ , and loose, strict underlay effectiveness  $Und_l \uparrow, Und_s \uparrow$ ; **Content metrics** include non-salient space utilization  $Uti \uparrow$ , salient space occlusion  $Occ \downarrow$ , and readability  $Rea \downarrow$ . Moreover, we newly proposed two content metrics, design intent *coverage*  $Cov \uparrow$  and *conflict*  $Con \downarrow$ , based on a design intent detection model  $\mathcal{S}_{pc}$  that is compreh-

Method	<i>Ove</i> $\downarrow$	<i>Ali</i> $\downarrow$	<i>Undi</i> $\uparrow$	<i>Unds</i> $\uparrow$	<i>Int</i> $\downarrow$	<i>Sal</i> $\downarrow$	<i>Rea</i> $\downarrow$	<i>Avg</i> $\downarrow$	
<b>Annotated Test Split</b>									
Non-LLM	<i>Real data</i>	0.0010	0.0038	0.9942	0.9903	0.0289	0.0368	0.0109	0.0138
	CGL-GAN	0.0966	0.0035	0.7854	0.3570	0.1204	0.2774	0.0191	0.1964
	DS-GAN	<b>0.0261</b>	0.0038	0.8350	<b>0.5804</b>	<b>0.0677</b>	0.3100	0.0199	<b>0.1446</b>
	ICVT	0.2572	0.0405	0.5384	0.3932	0.7831	1.0836	0.0259	0.4655
	LayoutDM <sup>†</sup>	0.1562	<b>0.0018</b>	0.6426	0.3873	0.5066	<b>0.2429</b>	0.0185	0.2709
	RALF	<b>0.0084</b>	0.0028	<b>0.9808</b>	<b>0.9201</b>	0.1162	<b>0.0479</b>	<b>0.0128</b>	<b>0.0410</b>
LLM-based	<i>Tuning-required</i>								
	PosterLlama <sup>‡</sup>	0.0008	0.0006	0.9999	0.9982	0.3407	0.2619	0.0177	0.0891
	<i>Tuning-free</i>								
	LayoutPrompter <sub>L2</sub>	0.0083	0.0030	0.3716	0.1633	0.3200	0.9433	0.0319	0.3959
	LayoutPrompter <sub>CL</sub>	0.0040	0.0030	0.4415	0.1937	0.3662	0.9035	0.0301	0.3817
	LayoutPrompter <sub>L3</sub>	0.0017	0.0028	0.4085	0.1613	0.5199	0.8567	0.0309	0.4060
	PosterO <sub>L2</sub> (Ours)	<b>0.0004</b>	0.0027	0.7597	0.5605	0.3679	<b>0.1491</b>	<b>0.0188</b>	0.1741
LLM-based	PosterO <sub>CL</sub> (Ours)	<b>0.0004</b>	0.0028	<b>0.9621</b>	<b>0.8606</b>	0.2397	0.2295	0.0189	<b>0.0955</b>
	PosterO <sub>L3</sub> (Ours)	0.0006	<b>0.0025</b>	<b>0.9888</b>	<b>0.9211</b>	<b>0.1080</b>	<b>0.1110</b>	<b>0.0171</b>	<b>0.0470</b>
<b>Unannotated Test Split</b>									
Non-LLM	<i>Train data</i>	0.0012	0.0027	0.9969	0.9900	0.0000	0.0000	0.0108	0.0040
	CGL-GAN	0.1010	0.0048	0.7326	0.2743	<b>0.2275</b>	0.7755	0.0327	0.3049
	DS-GAN	<b>0.0248</b>	0.0046	<b>0.7859</b>	<b>0.4676</b>	<b>0.1659</b>	0.5868	0.0320	<b>0.2229</b>
	ICVT	0.2786	0.0480	0.4939	0.3549	0.7947	1.3289	0.0347	0.5194
	LayoutDM <sup>†</sup>	0.1638	<b>0.0029</b>	0.5987	0.3695	0.5357	<b>0.3172</b>	0.0264	0.2968
	RALF	<b>0.0175</b>	0.0069	<b>0.9548</b>	<b>0.8653</b>	0.5986	<b>0.1779</b>	<b>0.0231</b>	<b>0.1434</b>
LLM-based	<i>Tuning-required</i>								
	PosterLlama <sup>‡</sup>	0.0006	0.0006	0.9986	0.9917	0.2667	0.3823	0.0285	0.0983
	<i>Tuning-free</i>								
	LayoutPrompter <sub>L2</sub>	0.0095	0.0032	0.3401	0.1161	0.5349	1.2050	0.0408	0.4767
	LayoutPrompter <sub>CL</sub>	0.0032	0.0028	0.4052	0.1464	0.5148	1.1106	0.0395	0.4456
	LayoutPrompter <sub>L3</sub>	0.0010	0.0026	0.4054	0.1621	0.7005	1.0838	0.0412	0.4660
	PosterO <sub>L2</sub> (Ours)	<b>0.0004</b>	0.0031	0.7284	0.5188	0.4030	<b>0.3351</b>	<b>0.0265</b>	0.2173

Table 1. Comparisons of quantitative results on PKU PosterLayout dataset.

hensively pre-trained on [19] and [55]. Calculating  $Cov \uparrow$  and  $Con \downarrow$  is similar to  $Uti \uparrow$  and  $Occ \downarrow$  but using the predicted intent maps. As reported in Tab. 2, intent maps have **doubled** the matched portion with real layout data, reduced the unmatched portion by **34.7%**, and required only **1.3%** computational costs. These findings have demonstrated that intent-aware metrics are more credible and efficient. For a holistic understanding, we standardize intent-aware and saliency-aware metrics to  $Int \downarrow$  and  $Sal \downarrow$ , as follows:

$$Int = \Sigma \left( \frac{|Cov_{\hat{L}} - Cov_L|}{1 - Cov_L}, \frac{|Con_{\hat{L}} - Con_L|}{Con_L} \right),$$

$$Sal = \Sigma \left( \frac{|Uti_{\hat{L}} - Uti_L|}{1 - Uti_L}, \frac{|Occ_{\hat{L}} - Occ_L|}{Occ_L} \right), \quad (2)$$

where  $L$  and  $\hat{L}$  are the layouts from the train split and generation. Finally, we introduce an average metric  $Avgc$ .

### 4.3. Implementation Details

To ensure independent evaluations on [19] and [55], we correspondingly train two detection models,  $\mathcal{S}_p$  and  $\mathcal{S}_c$ , with mean squared error loss and a learning rate of  $1e^{-6}$ . Each detection model is with a Transformer encoder tailored for

Prediction	PKU		CGL	
	Match $\uparrow$	Unmatch $\downarrow$	Match $\uparrow$	Unmatch $\downarrow$
Saliency map	0.2238	0.1193	0.1984	0.1352
Design intent map	<b>0.4414</b>	<b>0.0996</b>	<b>0.4036</b>	<b>0.0883</b>
Inference cost	Network architecture	#FLOPs(G)	#Params(M)	
Saliency map	ISNet + BASNet	287.83	131.11	
Design intent map	UNet (MiT-B1)	<b>3.74</b>	<b>16.43</b>	

Table 2. Comparisons of the predicted saliency and design intent maps on the *annotated test* splits of PKU PosterLayout and CGL datasets, showing that intent-aware metrics are more credible.

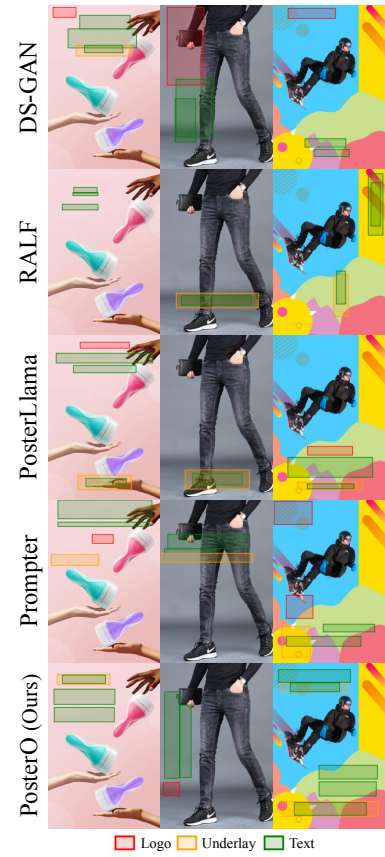


Figure 4. Comparisons of visualized results on the *unannotated test split* of PKU PosterLayout dataset.

semantic segmentation, MiT-B1 [51]. For in-context learning (ICL), we implement  $\mathcal{M}$  with three open-source LLMs, including Llama 2-7B ( $L2$ ) [47], CodeLlama-7B ( $CL$ ) [42], and Llama 3.1-8B ( $L3$ ) [11], with an unified sampling temperature of 0.7. Considering the context lengths and remaining consistent with LayoutPrompter [31], the example size  $k$  is 5, 10, and 10, respectively. Still adhering to [31], a layout ranker is employed, while mIoU in the quality function measures the similarity between generated layouts and predicted design intents rather than real data, minimizing the risk of data leakage.

Method	<i>Ove</i> $\downarrow$	<i>Ali</i> $\downarrow$	<i>Und<sub>t</sub></i> $\uparrow$	<i>Und<sub>s</sub></i> $\uparrow$	<i>Int</i> $\downarrow$	<i>Sal</i> $\downarrow$	<i>Rea</i> $\downarrow$	<i>Avg</i> $\downarrow$	
<b>Annotated Test Split</b>									
Non-LLM	<i>Real data</i>	0.0003	0.0024	0.9963	0.9880	0.0088	0.0097	0.0119	0.0070
	CGL-GAN	0.2291	0.0123	0.6466	0.2281	0.7088	0.4627	0.0213	0.3656
	DS-GAN	0.0460	<b>0.0022</b>	0.9081	0.6308	0.3950	0.1539	0.0181	0.1537
	ICVT	0.2453	0.0179	0.5150	0.3326	0.3632	0.5139	0.0211	0.3305
	LayoutDM <sup>†</sup>	0.0184	<b>0.0021</b>	0.9216	0.8159	0.0411	<b>0.0286</b>	<b>0.0137</b>	0.0523
	RALF	<b>0.0042</b>	0.0024	<b>0.9912</b>	<b>0.9756</b>	<b>0.0366</b>	0.0724	0.0180	<b>0.0238</b>
LLM-based	<i>Tuning-required</i>								
	PosterLlama <sup>‡</sup>	0.0006	0.0006	0.9987	0.9890	0.1337	0.2559	0.0184	0.0602
	<i>Tuning-free</i>								
	LayoutPrompter <sub>L2</sub>	0.0087	0.0033	0.3369	0.1455	0.3362	0.8234	0.0327	0.3888
	LayoutPrompter <sub>CL</sub>	0.0037	0.0031	0.3965	0.1616	0.3718	0.7799	0.0317	0.3760
	LayoutPrompter <sub>L3</sub>	0.0017	0.0030	0.3830	0.1740	0.5593	0.7957	0.0327	0.4051
	PosterO <sub>L2</sub> (Ours)	<b>0.0006</b>	<b>0.0023</b>	0.7801	0.6150	0.2542	<b>0.0467</b>	0.0176	0.1323
LLM-based	PosterO <sub>CL</sub> (Ours)	<b>0.0005</b>	<b>0.0023</b>	0.9682	<b>0.8868</b>	0.1246	0.0700	<b>0.0168</b>	<b>0.0513</b>
	PosterO <sub>L3</sub> (Ours)	0.0006	<b>0.0022</b>	<b>0.9842</b>	<b>0.9340</b>	<b>0.0388</b>	<b>0.0026</b>	<b>0.0161</b>	<b>0.0203</b>
Non-LLM	<b>Unannotated Test Split</b>								
	<i>Train data</i>	0.0003	0.0027	0.9945	0.9858	0.0000	0.0000	0.0118	0.0049
	CGL-GAN	0.2668	0.0316	0.6774	0.1656	<b>0.9707</b>	2.3973	<b>0.0512</b>	0.6964
	DS-GAN	0.0991	<b>0.0138</b>	<b>0.7566</b>	0.2810	<b>0.4607</b>	<b>2.2732</b>	0.0526	<b>0.5517</b>
	ICVT	0.2045	0.1010	0.4357	0.2599	1.2813	2.6512	<b>0.0397</b>	0.7974
	LayoutDM <sup>†</sup>	0.0793	0.1822	0.6304	0.3853	1.5002	3.2906	0.0612	0.8711
	RALF	<b>0.0273</b>	0.0189	<b>0.9756</b>	<b>0.9315</b>	1.0237	<b>1.6798</b>	<b>0.0397</b>	<b>0.4118</b>
LLM-based	<i>Tuning-required</i>								
	PosterLlama <sup>‡</sup>	0.0014	0.0007	0.9971	0.9771	0.3510	2.6170	0.0555	0.4359
	<i>Tuning-free</i>								
	LayoutPrompter <sub>L2</sub>	0.0069	0.0103	0.2847	0.1126	1.0257	2.3702	0.0628	0.7255
	LayoutPrompter <sub>CL</sub>	0.0045	0.0024	0.3239	0.1341	1.5800	2.5380	0.0650	0.8188
	LayoutPrompter <sub>L3</sub>	0.0026	<b>0.0016</b>	0.2693	0.1142	1.6249	2.4128	0.0644	0.8175
	PosterO <sub>L2</sub> (Ours)	0.0005	0.0033	0.6663	0.4770	<b>0.3522</b>	<b>1.2365</b>	0.0382	0.3553
LLM-based	PosterO <sub>CL</sub> (Ours)	<b>0.0003</b>	0.0037	0.9369	<b>0.8071</b>	<b>0.2771</b>	1.3223	<b>0.0379</b>	0.2710
	PosterO <sub>L3</sub> (Ours)	0.0004	0.0032	<b>0.9816</b>	<b>0.9034</b>	0.4328	<b>1.2407</b>	<b>0.0365</b>	<b>0.2612</b>

Table 3. Comparisons of quantitative results on CGL dataset.

#### 4.4. Comparison with State-of-the-arts

We select approaches with open-sourced implementation as baselines, including GAN-based CGL-GAN [55], DS-GAN [19], auto-regression-based ICVT [4], RALF [17], diffusion model-based LayoutDM<sup>†</sup> [21], and also LLM-based PosterLlama<sup>‡</sup> [44], LayoutPrompter [31].

**Baseline comparison.** Tab. 1 reports the quantitative results on PKU PosterLayout. The proposed PosterO shows the best overall performance across the test splits. Particularly, when confronting the challenging unannotated split that poses domain adaptation problems [52], it still achieves new *state-of-the-art* (SOTA) results with outstanding stability. Compared to the current non-LLM and LLM-based SOTA approaches, *i.e.*, RALF and PosterLlama, ours significantly improves the average metric *Avg*  $\downarrow$  by 52.8% and 31.1%. Consistent results are obtained on CGL, as reported in Tab. 3, ours improves *Avg*  $\downarrow$  by 36.6% and 40.1%.

More precisely, PosterO shows impressive graphic metrics (2<sup>nd</sup> column), closely resembling the distribution of real data, with only a slight deficit in the *Ali*  $\downarrow$  metric on the

unannotated split of CGL compared to LayoutPrompter. As for content metrics (3<sup>rd</sup> column), although PosterO uses only a small design intent detection model  $\mathcal{S}$ , it achieves comparable or even superior results to the baselines that utilize larger saliency detection models [26, 40] or costly fine-tuned DINOv2 [36]. Especially, PosterO is best at dealing with the *spatial shifts in subject distributions* [17] present in the unannotated split of CGL, maintaining an overwhelming lead in content metrics.

**Backbone LLMs  $\mathcal{M}$ .** Comparing the performance of tuning-free approaches across various LLMs is crucial for realizing how effectively the layout knowledge implicit in  $\mathcal{M}$  has been leveraged. As reported in Tab. 1 and Tab. 3, PosterO demonstrates overwhelming superiority over LayoutPrompter in all counterparts with the same  $\mathcal{M}$ . More importantly, from PosterO<sub>L2,CL</sub>, to PosterO<sub>L3</sub>, it is evident that the proposed approach has experienced improvements as the capabilities of its based  $\mathcal{M}$  increased. This finding indicates that new knowledge, such as programming, introduced during model updates, has indeed been leveraged to generate layouts. With the continuous development of LLMs, PosterO is anticipated to keep its rising potential.

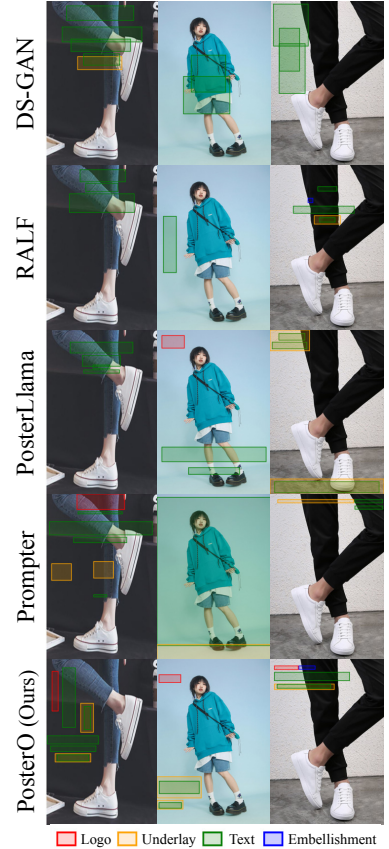


Figure 5. Comparisons of visualized results on the *unannotated test split* on CGL dataset.

<sup>†</sup>The extended version presented in [17].

<sup>‡</sup>With the released weights tuned on [19], [55], and synthesized data.

Method \ $k$	1	2	5	7	8	10
LayoutPrompter	0.7711	0.6690	0.5353	0.4883	0.4919	0.4660
PosterO (Ours)	0.0678	0.0746	0.0732	<u>0.0663</u>	<b>0.0651</b>	0.0677

Table 4. Comparisons of  $Avg \downarrow$  over in-context example size  $k$ .

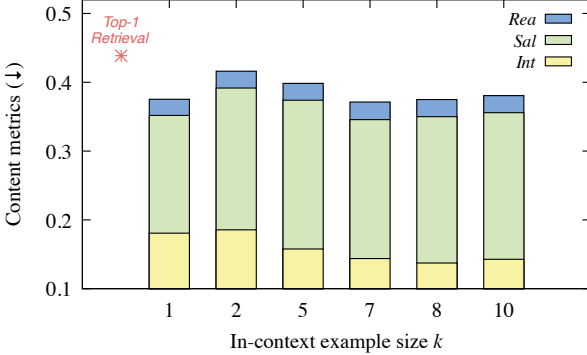


Figure 6. Content metrics over in-context example size  $k$ .

**Visualized results.** Fig. 4 and Fig. 5 show the layouts generated by different approaches. The results illustrate that PosterO generates high-quality layouts that the distribution of elements is generous and coordinated. In contrast, the approaches based on training or tuning tend to place elements centrally and thus fail to confront images with compositions that are less common in the training data. More visualized results are presented in supplementary material.

**In-context example size  $k$ .** To explore the impact of example selection during ICL, we test a set of candidates  $\{k\} = \{1, 2, 5, 7, 8, 10\}$  on the unannotated split of [19], as reported in Tab. 4. Amazingly, PosterO consistently outperforms LayoutPrompter and all other baselines in Tab. 1 across all settings of  $k$ . As the optimal performance occurs at  $k = 7$  and  $8$ , it is proved that  $\mathcal{M}$  has truly benefited from learning with the selected intent-aligned examples. To further observe how well these examples help  $\mathcal{M}$  understand visual contents, which is the focal point of content-aware layout generation, we plot the resultant content metrics over  $k$  in Fig. 6. It is noteworthy that directly adopting the most intent-aligned example (*Top-1 Retrieval*) surpasses all baselines, indicating a successful alignment between intent and layout in the latent space  $\mathbf{Z}_D$ . Nevertheless, we still observe improvements when involving in-context examples.

#### 4.5. Ablation Study

To investigate our design choice in layout tree construction (Sec. 3.1) and learning example selection (Sec. 3.2), as well as to explore PosterO’s adaptability to customized design intents and small-scale LLMs, we conducted the following ablation studies, mainly on the unannotated split of [19].

**Design choices for layout tree construction.** We investigate the effectiveness of the design intent vectorization ( $d$ ) and hierarchical node representation ( $h$ ) during constructing layout trees, as reported in Tab. 5. Due to space constraints,

$d$	$h$	$Und_l \uparrow$	$Und_s \uparrow$	$Int \downarrow$	$Sal \downarrow$	$Rea \downarrow$	$Avg \downarrow$
✓	✓	<b>0.9856</b>	<b>0.9241</b>	0.1427	0.2131	0.0248	<b>0.0677</b>
✓		0.8609	0.6650	<b>0.0981</b>	<b>0.1560</b>	<b>0.0240</b>	0.1078
	✓	0.9497	0.8836	0.9858	0.3991	0.0274	0.2260
		0.7628	0.6413	0.8162	0.2729	0.0246	0.2447

Table 5. Ablation study on the ( $d$ ) design intent vectorization and ( $h$ ) hierarchical node representation in layout tree construction.

Selection	$Und_l \uparrow$	$Und_s \uparrow$	$Int \downarrow$	$Sal \downarrow$	$Rea \downarrow$	$Avg \downarrow$
$f$ -aligned	0.9856	0.9241	<b>0.1427</b>	<b>0.2131</b>	0.0248	<b>0.0677</b>
$D$ -aligned	0.9866	0.9297	0.2221	0.2531	<b>0.0236</b>	0.0836
$E$ -aligned	0.9743	0.9026	0.3431	0.4177	0.0264	0.1304
Random	<b>0.9885</b>	<b>0.9302</b>	0.3225	0.4688	0.0295	0.1293

Table 6. Ablation study on different references for in-context example selection. ( $f$ : Embeddings of design intents,  $D$ : Bounding boxes of design intents,  $E$ : Sets of element types.)

$Ove \downarrow$  and  $Ali \downarrow$  are omitted, considering their slight fluctuations. As observed, the combination of  $d$  and  $h$  yields the best results. Although removing  $h$  appears to improve content metrics, this is primarily because the invalid empty underlays artificially inflate the utilization rate, as analyzed in supplementary material. The significant decreases witnessed in underlay effectiveness,  $Und_l$ ,  $Und_s$ , by up to 28%, further underscore this issue. In contrast, removing  $d$  from both the examples and postscript makes LLMs blindly mimic the provided instances. Here, however, shows a  $Sal \downarrow$  surpasses some baselines, such as CGL-GAN, DS-GAN, and LayoutPrompter, while  $Int \downarrow$  fails far behind, reflecting the robustness of the newly proposed metric  $Int \downarrow$ . If both  $d$  and  $h$  are removed, the most severe degradation is observed, up to 261%. In this way, we demonstrate the necessity of these design choices.

**Design choices for in-context example selection.** We have seen the remarkable performance of design intent embeddings  $f$ -aligned example selection, which relies on the learned latent space  $\mathbf{Z}_D$ . To investigate alternative references, we have considered bounding boxes of design intents ( $D$ -aligned), sets of element types ( $E$ -aligned), and even with no specific alignment (Random). As reported in Tab. 6, although all  $D$ -aligned,  $E$ -aligned, and random selections make declines in average metrics, the outcomes are still superior to most baseline approaches. In particular, using  $D$ -aligned selection also achieves a new SOTA result, which supports its eligibility as an alternative enabling PosterO to deliver acceptable content-aware layouts when faced with roughly sketched  $D$  from users.

**Adaption to customized design intent.** Upon the discussions from the previous paragraph, we take a further step to verify PosterO’s adaptability to customized design intents. Fig. 7 demonstrates the results of using the original  $D$  predicted by the detection model  $\mathcal{S}$  and three customized  $D$  with different levels of complexity. As the input  $D$  varies,

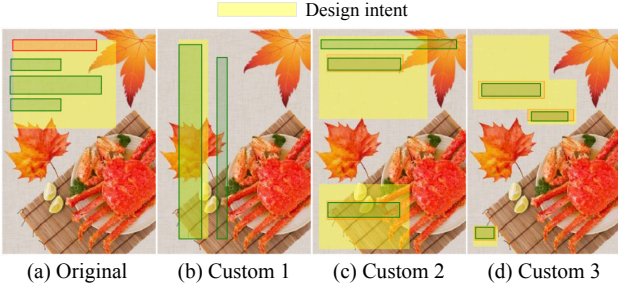


Figure 7. PosterO’s adaptability to different design intents  $D$ .

Method	$Und_t \uparrow$	$Und_s \uparrow$	$Int \downarrow$	$Sal \downarrow$	$Rea \downarrow$	$Avg \downarrow$
<b>Annotated Test Split of PKU PosterLayout</b>						
Ours <sub>L3-8B</sub>	0.9888	0.9211	0.1080	0.1110	0.0171	0.0470
Ours <sub>L3.2-1B</sub>	0.9159	0.6871	0.2633	<b>0.1026</b>	0.0174	0.1119
Ours <sub>L3.2-3B</sub>	0.9662	0.8595	0.2166	0.1400	<b>0.0168</b>	0.0787
<b>Unannotated Test Split of PKU PosterLayout</b>						
Ours <sub>L3-8B</sub>	0.9856	0.9241	0.1427	0.2131	0.0248	0.0677
Ours <sub>L3.2-1B</sub>	0.9008	0.6643	0.2702	0.2910	0.0276	0.1467
Ours <sub>L3.2-3B</sub>	0.9731	0.8724	0.2276	0.2479	0.0249	0.0940
<b>Annotated Test Split of CGL</b>						
Ours <sub>L3-8B</sub>	0.9842	0.9340	0.0388	0.0026	0.0161	0.2023
Ours <sub>L3.2-1B</sub>	0.9222	0.7724	0.1467	0.0463	0.0169	0.0741
Ours <sub>L3.2-3B</sub>	0.9677	0.8784	0.0469	0.0118	0.0163	0.0331
<b>Unannotated Test Split of CGL</b>						
Ours <sub>L3-8B</sub>	<b>0.9816</b>	0.9034	0.4328	1.2407	0.0365	0.2612
Ours <sub>L3.2-1B</sub>	0.8440	0.6409	<b>0.2868</b>	<b>1.1101</b>	0.0381	0.2791
Ours <sub>L3.2-3B</sub>	0.9682	0.8349	0.3191	1.1728	<b>0.0359</b>	<b>0.2469</b>

Table 7. Ablation study on  $\mathcal{M}$  accommodating small-scale LLMs.

PosterO dynamically adjusts the spatial distribution of elements in the generated layouts while maintaining remarkable graphic metrics. Notably, this capability is unique to PosterO, attributed to its intent-based paradigm.

**Adaption to small-scale backbone LLM  $\mathcal{M}$ .** To address resource-limited environments and to accelerate the layout generation process, we investigate PosterO’s adaptability to small-scale LLMs [35], including Llama3.2-1B ( $L3.2-1B$ ) and Llama3.2-3B ( $L3.2-3B$ ). As reported in Tab. 7, PosterO maintains very competitive and or even better results with the smaller  $\mathcal{M}$ , showcasing its potential for more flexible and efficient applications.

#### 4.6. Generalized Content-aware Layout Generation

To verify PosterO’s potential in generalized content-aware layout generation, which is presented for the first time in this work, we built a new dataset, **PStylish7**. It comprises 152 few-shot learning samples and 100 test images, covering seven poster categories. Each serves as a representative prototype for a segment in the spectrum of poster design purposes, encompassing artwork exhibition (*Paint*), cultural education (*Poem*), public safety (*Metro*), entertainment marketing (*Movie*), merchandising display (*Menu*), public advocacy (*Animal*), and social-media interaction (*Instagram*). Besides, it covers eight element types, including

Ours <sub>CL</sub>	Paint	Poem	Metro	Movie	Menu	Animal	Insta.
$Ove \downarrow$	0.0047	0.0034	<b>0.0618</b>	0.0106	0.0083	<b>0.0032</b>	0.0010
$Int \downarrow$	0.7690	<b>0.2198</b>	<b>0.6987</b>	<b>0.1216</b>	0.2359	<b>0.3020</b>	<b>0.2674</b>
$Sal \downarrow$	3.8838	0.8484	1.3604	0.3275	0.7191	<b>2.6280</b>	<b>0.6652</b>
$Avg \downarrow$	1.5525	0.3572	0.7070	<b>0.1532</b>	0.3211	<b>0.9777</b>	<b>0.3112</b>
Ours <sub>L3</sub>	Paint	Poem	Metro	Movie	Menu	Animal	Insta.
$Ove \downarrow$	<b>0.0032</b>	<b>0.0028</b>	0.0777	<b>0.0004</b>	<b>0.0056</b>	0.1495	<b>0.0004</b>
$Int \downarrow$	<b>0.6219</b>	0.6274	0.7478	0.3375	<b>0.1620</b>	0.5383	1.1431
$Sal \downarrow$	<b>2.4512</b>	<b>0.1600</b>	<b>1.1111</b>	<b>0.1347</b>	<b>0.5790</b>	2.9284	1.0810
$Avg \downarrow$	<b>1.0254</b>	<b>0.2634</b>	<b>0.6455</b>	0.1575	<b>0.2489</b>	1.2054	0.7415

Table 8. Quantitative results on PStylish7 dataset.

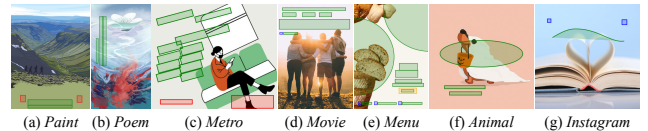


Figure 8. Visualized results on PStylish7 dataset.

all those in the existing datasets and four text variants depicted in Sec. 3.1. Considering feasibility, we employ five metrics, including  $Ove \downarrow$ , ( $Cov \uparrow$ ,  $Con \downarrow$ ), standardized as  $Int \downarrow$ , and ( $Uti \uparrow$ ,  $Occ \downarrow$ ), standardized as  $Sal \downarrow$ . More details about PStylish7 are given in supplementary material.

The quantitative results are reported in Tab. 8, and the visualized results are presented in Fig. 8. Here, the detection model  $S_{pc}$  is employed to obtain design intents  $D$  and their features  $f$ . While PosterO<sub>L3</sub> outperforms PosterO<sub>CL</sub> in most categories, as the first attempt in this field, there is still plenty of room for improvement. Overall, the proposed PStylish7 is significantly more challenging than the existing datasets, attributed to its broader and sparser data distribution. This requires approaches with good generalization capabilities, mirroring real-world scenarios, and can stimulate more advanced work in the future.

## 5. Conclusion and Discussion

This work presented a tuning-free language model-based approach for content-aware layout generation, named **PosterO**. Through extensive experiments, we demonstrated that PosterO achieves new state-of-the-art results on various benchmarks, mainly attributed to the structural representation, *layout trees*. Moreover, we delved into the task under *generalized* settings and built the first available dataset, **PStylish7**, which covers seven poster purposes and eight element types. Employing PStylish7, we verified PosterO’s potential to solve complicated tasks in real-world scenarios, underscoring its practicality. The future work mainly lies in two aspects. First, enhancing the generalized capabilities of layout generation approaches is highly valuable, as PosterO aims. With the challenging test offered by the proposed PStylish7 dataset, it is increasingly attainable. Second, integrating feedback mechanisms is envisioned to facilitate self-optimization and allow the incorporation of user suggestions, forming a more interactive, user-centric process.

## Acknowledgments

This work was supported by the National Natural Science Foundation of China (61925201, 62132001, 62432001) and Beijing Natural Science Foundation (L247006).

## References

- [1] Diego Martin Arroyo, Janis Postels, and Federico Tombari. Variational transformer networks for layout generation. In *Proceedings of the IEEE/CVF Conference on Computer Vision and Pattern Recognition*, pages 13642–13652, 2021. [2](#)
- [2] Canva. Visual economy report 2024 edition: How visual communication fuels new business opportunities. <https://www.canva.com/visual-economy-report/>, 2024. [1](#)
- [3] Canva. 10 highlights from canva create 2024: Redesigned for work. <https://www.canva.com/newsroom/news/what-happened-at-canva-create-2024/>, 2024. [1](#)
- [4] Yunning Cao, Ye Ma, Min Zhou, Chuanbin Liu, Hongtao Xie, Tiezheng Ge, and Yuning Jiang. Geometry aligned variational transformer for image-conditioned layout generation. In *Proceedings of the ACM International Conference on Multimedia*, pages 1561–1571, 2022. [1, 2, 6](#)
- [5] Yunning Cao, Chuanbin Liu, Ye Ma, Min Zhou, Tiezheng Ge, Yuning Jiang, and Hongtao Xie. Self-refined variational transformer for image-conditioned layout generation. *International Journal of Machine Learning and Cybernetics*, pages 1–18, 2024. [2](#)
- [6] Shang Chai, Liansheng Zhuang, and Fengying Yan. Layoutdm: Transformer-based diffusion model for layout generation. In *Proceedings of the IEEE/CVF Conference on Computer Vision and Pattern Recognition*, pages 18349–18358, 2023. [2](#)
- [7] Shang Chai, Liansheng Zhuang, Fengying Yan, and Zihan Zhou. Two-stage content-aware layout generation for poster designs. In *Proceedings of the ACM International Conference on Multimedia*, pages 8415–8423, 2023. [1, 2](#)
- [8] Jian Chen, Ruiyi Zhang, Yufan Zhou, Jennifer Healey, Jiuxiang Gu, Zhiqiang Xu, and Changyou Chen. Textlap: Customizing language models for text-to-layout planning. In *Proceedings of the Conference on Empirical Methods in Natural Language Processing: Findings*, 2024. [2](#)
- [9] Erik Dahlström, Anthony Grasso, Niklas Hagelroth, Chris Lilley, Cameron McCormack, and Doug Schepers. Scalable vector graphics (svg) 2.0 specification. svg working group, w3c. <https://dev.w3.org/SVG/profiles/2.0/publish/>, 2002. [2, 3](#)
- [10] Leichao Dai, Lin Feng, Xinglin Shang, and Han Su. Cross modal adaptive few-shot learning based on task dependence. *Chinese Journal of Electronics*, 32(1):85–96, 2023. [2](#)
- [11] Abhimanyu Dubey, Abhinav Jauhri, Abhinav Pandey, Abhishek Kadian, Ahmad Al-Dahle, Aiesha Letman, Akhil Mathur, Alan Schelten, Amy Yang, Angela Fan, et al. The llama 3 herd of models. *arXiv preprint arXiv:2407.21783*, 2024. [1, 2, 5](#)
- [12] Weixi Feng, Wanrong Zhu, Tsu-jui Fu, Varun Jampani, Arjun Akula, Xuehai He, Sugato Basu, Xin Eric Wang, and William Yang Wang. Layoutgpt: Compositional visual planning and generation with large language models. *Proceedings of the International Conference on Neural Information Processing Systems*, 36, 2024. [1, 2](#)
- [13] Stephanie Fu, Netanel Tamir, Shobhita Sundaram, Lucy Chai, Richard Zhang, Tali Dekel, and Phillip Isola. Dreamsim: Learning new dimensions of human visual similarity using synthetic data. In *Proceedings of the International Conference on Neural Information Processing Systems*, pages 50742–50768, 2024. [2](#)
- [14] Shunan Guo, Zhuochen Jin, Fuling Sun, Jingwen Li, Zhaorui Li, Yang Shi, and Nan Cao. Vinci: an intelligent graphic design system for generating advertising posters. In *Proceedings of the CHI Conference on Human Factors in Computing Systems*, pages 1–17, 2021. [2](#)
- [15] Kamal Gupta, Justin Lazarow, Alessandro Achille, Larry S Davis, Vijay Mahadevan, and Abhinav Shrivastava. Layout-transformer: Layout generation and completion with self-attention. In *Proceedings of the IEEE/CVF International Conference on Computer Vision*, pages 1004–1014, 2021. [2](#)
- [16] Sun Haoran, Wang Yang, Liu Haipeng, and Qian Biao. Fine-grained cross-modal fusion based refinement for text-to-image synthesis. *Chinese Journal of Electronics*, 32(6):1329–1340, 2023. [2](#)
- [17] Daichi Horita, Naoto Inoue, Kotaro Kikuchi, Kota Yamaguchi, and Kiyoharu Aizawa. Retrieval-augmented layout transformer for content-aware layout generation. In *Proceedings of the IEEE/CVF Conference on Computer Vision and Pattern Recognition*, pages 67–76, 2024. [1, 2, 4, 6](#)
- [18] HsiaoYuan Hsu, Xiangteng He, and Yuxin Peng. Densitylayout: Density-conditioned layout gan for visual-textual presentation designs. In *Proceedings of the International Conference on Image and Graphics*, pages 187–199, 2023. [1, 2, 3](#)
- [19] HsiaoYuan Hsu, Xiangteng He, Yuxin Peng, Hao Kong, and Qing Zhang. Posterlayout: A new benchmark and approach for content-aware visual-textual presentation layout. In *Proceedings of the IEEE/CVF Conference on Computer Vision and Pattern Recognition*, pages 6018–6026, 2023. [1, 2, 4, 5, 6, 7](#)
- [20] Edward J Hu, Yelong Shen, Phillip Wallis, Zeyuan Allen-Zhu, Yuanzhi Li, Shean Wang, Lu Wang, and Weizhu Chen. Lora: Low-rank adaptation of large language models. *arXiv preprint arXiv:2106.09685*, 2021. [2](#)
- [21] Naoto Inoue, Kotaro Kikuchi, Edgar Simo-Serra, Mayu Otani, and Kota Yamaguchi. Layoutdm: Discrete diffusion model for controllable layout generation. In *Proceedings of the IEEE/CVF Conference on Computer Vision and Pattern Recognition*, pages 10167–10176, 2023. [6, 2](#)
- [22] Chao Jia, Yinfei Yang, Ye Xia, Yi-Ting Chen, Zarana Parekh, Hieu Pham, Quoc Le, Yun-Hsuan Sung, Zhen Li, and Tom Duerig. Scaling up visual and vision-language representation learning with noisy text supervision. In *Proceedings of the International Conference on Machine Learning*, pages 4904–4916, 2021. [1](#)
- [23] Kotaro Kikuchi, Edgar Simo-Serra, Mayu Otani, and Kota Yamaguchi. Constrained graphic layout generation via la

- tent optimization. In *Proceedings of the ACM International Conference on Multimedia*, pages 88–96, 2021. 2
- [24] Suhas Kotha, Jacob Mitchell Springer, and Aditi Raghunathan. Understanding catastrophic forgetting in language models via implicit inference. In *The Twelfth International Conference on Learning Representations*, 2024. 4
- [25] Hsin-Ying Lee, Lu Jiang, Irfan Essa, Phuong B Le, Haifeng Gong, Ming-Hsuan Yang, and Weilong Yang. Neural design network: Graphic layout generation with constraints. In *Proceedings of the European Conference on Computer Vision*, pages 491–506, 2020. 2
- [26] Chenhui Li, Peiying Zhang, and Changbo Wang. Harmonious textual layout generation over natural images via deep aesthetics learning. *IEEE Transactions on Multimedia*, 2021. 2, 6
- [27] Fengheng Li, An Liu, Wei Feng, Honghe Zhu, Yaoyu Li, Zheng Zhang, Jingjing Lv, Xin Zhu, Junjie Shen, Zhangang Lin, et al. Relation-aware diffusion model for controllable poster layout generation. In *Proceedings of the ACM International Conference on Information and Knowledge Management*, pages 1249–1258, 2023. 2
- [28] Jianan Li, Jimei Yang, Aaron Hertzmann, Jianming Zhang, and Tingfa Xu. LayoutGAN: Synthesizing graphic layouts with vector-wireframe adversarial networks. *IEEE Transactions on Pattern Analysis and Machine Intelligence*, 43(7): 2388–2399, 2020. 2
- [29] Jianan Li, Jimei Yang, Jianming Zhang, Chang Liu, Christina Wang, and Tingfa Xu. Attribute-conditioned layout GAN for automatic graphic design. *IEEE Transactions on Visualization and Computer Graphics*, 27(10):4039–4048, 2020. 2
- [30] Yinan Li, Jia Chen, Yin Bai, Jia Cheng, and Jun Lei. Design element aware poster layout generation. In *Proceedings of the ACM International Conference on Information and Knowledge Management*, pages 1296–1305, 2024. 2
- [31] Jiawei Lin, Jiaqi Guo, Shizhao Sun, Zijiang Yang, Jian-Guang Lou, and Dongmei Zhang. Layoutprompter: Awaken the design ability of large language models. In *Proceedings of the International Conference on Neural Information Processing Systems*, pages 43852–43879, 2023. 1, 2, 5, 6
- [32] Jinpeng Lin, Min Zhou, Ye Ma, Yifan Gao, Chenxi Fei, Yangjian Chen, Zhang Yu, and Tiezheng Ge. Autoposter: A highly automatic and content-aware design system for advertising poster generation. In *Proceedings of the ACM International Conference on Multimedia*, pages 1250–1260, 2023. 1, 2
- [33] Yun Luo, Zhen Yang, Fandong Meng, Yafu Li, Jie Zhou, and Yue Zhang. An empirical study of catastrophic forgetting in large language models during continual fine-tuning. *arXiv preprint arXiv:2308.08747*, 2023. 4
- [34] Ben Mann, N Ryder, M Subbiah, J Kaplan, P Dhariwal, A Neelakantan, P Shyam, G Sastry, A Askell, S Agarwal, et al. Language models are few-shot learners. In *Proceedings of the International Conference on Neural Information Processing Systems*, pages 1877–1901, 2020. 4
- [35] Meta. Llama 3.2: Revolutionizing edge ai and vision with open, customizable models. <https://ai.meta.com/blog/llama-3-2-connect-2024-vision-edge-mobile-devices/>, 2024. 2, 8
- [36] Maxime Oquab, Timothée Darcet, Théo Moutakanni, Huy Vo, Marc Szafraniec, Vasil Khalidov, Pierre Fernandez, Daniel Haziza, Francisco Massa, Alaeldin El-Nouby, et al. Dinov2: Learning robust visual features without supervision. *arXiv preprint arXiv:2304.07193*, 2023. 2, 6
- [37] Long Ouyang, Jeffrey Wu, Xu Jiang, Diogo Almeida, Carroll Wainwright, Pamela Mishkin, Chong Zhang, Sandhini Agarwal, Katarina Slama, Alex Ray, et al. Training language models to follow instructions with human feedback. In *Proceedings of the International Conference on Neural Information Processing Systems*, pages 27730–27744, 2022. 1
- [38] Yi-Hao Peng, Faria Huq, Yue Jiang, Jason Wu, Amanda Xin Yue Li, Jeffrey Bigham, and Amy Pavel. Dreamstruct: Understanding slides and user interfaces via synthetic data generation. In *Proceedings of the European Conference on Computer Vision*, 2024. 2
- [39] Xuebin Qin, Zichen Zhang, Chenyang Huang, Chao Gao, Masood Dehghan, and Martin Jaggersand. Basnet: Boundary-aware salient object detection. In *Proceedings of the IEEE/CVF Conference on Computer Vision and Pattern Recognition*, pages 7479–7489, 2019. 2
- [40] Xuebin Qin, Hang Dai, Xiaobin Hu, Deng-Ping Fan, Ling Shao, and Luc Van Gool. Highly accurate dichotomous image segmentation. In *Proceedings of the European Conference on Computer Vision*, pages 38–56, 2022. 2, 6
- [41] Olaf Ronneberger, Philipp Fischer, and Thomas Brox. U-net: Convolutional networks for biomedical image segmentation. In *Proceedings of the International Conference On Medical Image Computing and Computer Assisted Intervention*, pages 234–241, 2015. 3
- [42] Baptiste Roziere, Jonas Gehring, Fabian Gloclekle, Sten Sootla, Itai Gat, Xiaoqing Ellen Tan, Yossi Adi, Jingyu Liu, Romain Sauvestre, Tal Remez, et al. Code llama: Open foundation models for code. *arXiv preprint arXiv:2308.12950*, 2023. 1, 2, 5
- [43] Christoph Schuhmann, Romain Beaumont, Richard Vencu, Cade Gordon, Ross Wightman, Mehdi Cherti, Theo Coombes, Aarush Katta, Clayton Mullis, Mitchell Wortsman, et al. Laion-5b: An open large-scale dataset for training next generation image-text models. In *Proceedings of the International Conference on Neural Information Processing Systems*, pages 25278–25294, 2022. 1
- [44] Jaejung Seol, Seojun Kim, and Jaejun Yoo. Posterllama: Bridging design ability of language model to content-aware layout generation. In *Proceedings of the European Conference on Computer Vision*, pages 451–468, 2024. 1, 2, 6
- [45] Roman Suvorov, Elizaveta Logacheva, Anton Mashikhin, Anastasia Remizova, Arsenii Ashukha, Aleksei Silvestrov, Naejin Kong, Harshith Goka, Kiwoong Park, and Victor Lempitsky. Resolution-robust large mask inpainting with fourier convolutions. In *Proceedings of the IEEE/CVF WInter Conference on Applications of Computer Vision*, pages 2149–2159, 2022. 2
- [46] Zecheng Tang, Chenfei Wu, Juntao Li, and Nan Duan. Layoutnuwa: Revealing the hidden layout expertise of large language models. *Proceedings of International Conference on Learning Representations*, 2024. 1, 2

- [47] Hugo Touvron, Louis Martin, Kevin Stone, Peter Albert, Amjad Almahairi, Yasmine Babaee, Nikolay Bashlykov, Soumya Batra, Prajwal Bhargava, Shruti Bhosale, et al. Llama 2: Open foundation and fine-tuned chat models. *arXiv preprint arXiv:2307.09288*, 2023. [1](#), [2](#), [5](#)
- [48] Bo Wang, Quan Chen, Min Zhou, Zhiqiang Zhang, Xiaogang Jin, and Kun Gai. Progressive feature polishing network for salient object detection. In *Proceedings of the AAAI Conference on Artificial Intelligence*, pages 12128–12135, 2020. [2](#)
- [49] Shaodong Wang, Yunyang Ge, Liuhan Chen, Haiyang Zhou, Qian Wang, Xinhua Cheng, and Li Yuan. Prompt2poster: Automatically artistic chinese poster creation from prompt only. In *Proceedings of the ACM International Conference on Multimedia*, pages 10716–10724, 2024. [1](#), [2](#)
- [50] Haohan Weng, Danqing Huang, Yu Qiao, Zheng Hu, Chin-Yew Lin, Tong Zhang, and CL Chen. Desigen: A pipeline for controllable design template generation. In *Proceedings of the IEEE/CVF Conference on Computer Vision and Pattern Recognition*, pages 12721–12732, 2024. [1](#), [2](#)
- [51] Enze Xie, Wenhui Wang, Zhiding Yu, Anima Anandkumar, Jose M Alvarez, and Ping Luo. Segformer: Simple and efficient design for semantic segmentation with transformers. In *Proceedings of the International Conference on Neural Information Processing Systems*, pages 12077–12090, 2021. [5](#)
- [52] Chenchen Xu, Min Zhou, Tiezheng Ge, Yuning Jiang, and Weiwei Xu. Unsupervised domain adaption with pixel-level discriminator for image-aware layout generation. In *Proceedings of the IEEE/CVF Conference on Computer Vision and Pattern Recognition*, pages 10114–10123, 2023. [2](#), [6](#)
- [53] Tao Yang, Fan Wang, Junfan Lin, Zhongang Qi, Yang Wu, Jing Xu, Ying Shan, and Changwen Chen. Toward human perception-centric video thumbnail generation. In *Proceedings of the ACM International Conference on Multimedia*, pages 6653–6664, 2023. [1](#), [2](#)
- [54] Lvmin Zhang, Anyi Rao, and Maneesh Agrawala. Adding conditional control to text-to-image diffusion models. In *Proceedings of the IEEE/CVF International Conference on Computer Vision*, pages 3836–3847, 2023. [2](#)
- [55] Min Zhou, Chenchen Xu, Ye Ma, Tiezheng Ge, Yuning Jiang, and Weiwei Xu. Composition-aware graphic layout GAN for visual-textual presentation designs. In *Proceedings of the International Joint Conference on Artificial Intelligence*, pages 4995–5001, 2022. [1](#), [2](#), [4](#), [5](#), [6](#)
- [56] Deyao Zhu, Jun Chen, Xiaoqian Shen, Xiang Li, and Mohamed Elhoseiny. Minigpt-4: Enhancing vision-language understanding with advanced large language models. *arXiv preprint arXiv:2304.10592*, 2023. [2](#)

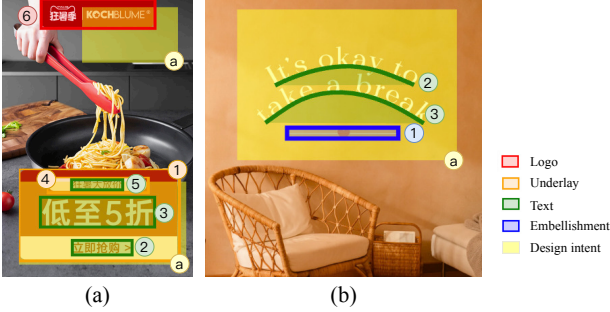
# PosterO: Structuring Layout Trees to Enable Language Models in Generalized Content-Aware Layout Generation

## Supplementary Material

This supplementary material provides additional information about the proposed approach, **PosterO**, and the new dataset, **PStylish7**. Sec. A presents examples of layout trees  $T$  and prompts  $P$ , Sec. B reports additional experimental results, and Sec. C provides more details and statistics about the PStylish7 dataset.

### A. Examples of Layout Trees and Prompts

**Layout trees  $T$ .** Fig. A presents examples of layout trees structured as depicted in Sec. 3.1. In (a), two distinct areas ① are detected for its design intent, and the double-nested underlay elements (*i.e.*, ①-⑤) contribute to a layout tree depth of three, based on the proposed hierarchical node representation. In (b), the curved texts (*i.e.*, ②,③) are outlined using `<path>`, following universal element vectorization.



Layout tree of (a)

```
<svg width="513" height="750" xmlns="http://www.w3.org/2000/svg">
  ①<polyon id="available_area" points="47,491 492,491 492,714 47,714" />
  ②<polyon id="available_area" points="215,22 470,22 470,171 215,171" />
  <rect id="canvas_0" x="0" y="0" width="513" height="750" />
  <svg x="47" y="456">
    ①<rect id="underlay_1" x="0" y="0" width="427" height="248" />
    ②<rect id="text_2" x="142" y="193" width="159" height="39" />
    ③<rect id="text_3" x="57" y="77" width="304" height="80" />
    <svg x="74" y="22">
      ④<rect id="underlay_4" x="0" y="0" width="270" height="43" />
      ⑤<rect id="text_5" x="66" y="8" width="136" height="27" />
    </svg>
  ⑥<rect id="logo_6" x="106" y="0" width="303" height="79" />
</svg>
```

Layout tree of (b)

```
<svg width="513" height="513" xmlns="http://www.w3.org/2000/svg">
  ①<polyon id="available_area" points="60,19 465,19 465,297 60,297" />
  <rect id="canvas_0" x="0" y="0" width="513" height="513" />
  ①<rect id="embellishment_1" x="152" y="237" width="205" height="20" />
  ②<path id="text-curved_2" d="M 130 159 C 156 146 198 127 253 124
    C 300 121 342 139 386 158" />
  ③<path id="text-curved_3" d="M 112 228 C 148 203 183 169 254 172
    C 313 174 361 201 404 229" />
</svg>
```

Figure A. Examples of layout trees  $T$  from (a) PKU PosterLayout and (b) PStylish7 datasets.

**Prompts  $P$ .** Fig. B presents examples of prompts created as depicted in Sec. 3.2. The canvases' varying sizes demonstrate PosterO's adaptability to diverse aspect ratios.

### Prompt (a)

**Preface** The following are some scalable vector graphics (svg) allocating elements on the canvas.

Example 0: This svg uses canvas\_0 of size (513, 750) with available areas (45, 504, 441, 716, 66, 443, 195) to allocate { underlay\_1, text\_2, logo\_3, text\_4, text\_5 }.

```
<svg width="513" height="750" xmlns="http://www.w3.org/2000/svg">
  <polygon id="available_area" points="45,504 441,504 441,716 45,716" />
  <polygon id="available_area" points="66,443 443,443 443,195 66,195" />
  <rect id="canvas_0" x="0" y="0" width="513" height="750" />
  <svg x="179" y="638">
    <rect id="underlay_1" x="0" y="0" width="157" height="51" />
    <rect id="text_2" x="25" y="13" width="105" height="28" />
  </svg>
  <rect id="logo_3" x="30" y="18" width="146" height="38" />
  <rect id="text_4" x="75" y="110" width="365" height="38" />
  <rect id="text_5" x="80" y="502" width="379" height="68" />
</svg>
```

Example 1: This svg uses canvas\_0 of size (513, 750) with available areas (71, 541, 437, 705, 55, 40, 438, 224) to allocate { text\_1, text\_2, text\_3 }.

```
<svg width="513" height="750" xmlns="http://www.w3.org/2000/svg">
  <polygon id="available_area" points="71,541 437,541 437,705 71,705" />
  <polygon id="available_area" points="55,40 438,40 438,224 55,224" />
  <rect id="canvas_0" x="0" y="0" width="513" height="750" />
  <rect id="text_1" x="23" y="109" width="468" height="54" />
  <rect id="text_2" x="27" y="41" width="459" height="60" />
  <rect id="text_3" x="59" y="573" width="397" height="47" />
</svg>
...
```

First, learn from the examples and understand how this template works.

- Then, create a new one while following the rules:
1. The svg must be meaningful, which implies that empty, all-zero, or symbolic attributes are not allowed.
  2. `<rect>` is the only legal svg tag, and the inner `<rect>` must be within the outer `<svg>`.
  3. The id of `<rect>` must be unique and picked from {}.
  4. The position of `<rect>` should be clustered neatly in available areas while avoiding intersection. If intersected, `<rect>` should be resized or moved.

Final: This svg uses canvas\_0 of size (513, 750) with available areas (69, 502, 411, 703, 59, 35, 474, 210) to allocate { underlay\_1, text\_2, logo\_3, text\_4, text\_5 }.

### Prompt (b)

**Preface** The following are some scalable vector graphics (svg) allocating elements on the canvas.

Example 0: This svg uses canvas\_0 of size (513, 641) with available areas (33, 20, 455, 281) to allocate { text-curved\_1 }.

```
<svg width="513" height="641" xmlns="http://www.w3.org/2000/svg">
  <polygon id="available_area" points="33,20 455,20 455,281 33,281" />
  <rect id="canvas_0" x="0" y="0" width="513" height="641" />
  <path id="text-curved_1" d="M 51 139 C 86 124 131 113 167 112 C 240 109 261 145
    366 176 C 396 185 441 182 465 180" />
</svg>
```

Example 1: This svg uses canvas\_0 of size (513, 513) with available areas (33, 0, 478, 171) to allocate { embellishment\_1, embellishment\_2, text-curved\_3 }.

```
<svg width="513" height="513" xmlns="http://www.w3.org/2000/svg">
  <polygon id="available_area" points="33,0 478,0 478,171" />
  <rect id="canvas_0" x="0" y="0" width="513" height="513" />
  <rect id="embellishment_1" x="43" y="158" width="28" height="25" />
  <rect id="embellishment_2" x="447" y="158" width="27" height="28" />
  <path id="text-curved_3" d="M 85 164 C 112 148 152 124 189 122 C 306 117 367 191
    436 181" />
</svg>
...
```

First, learn from the examples and understand how this template works.

- Then, create a new one while following the rules:
1. The svg must be meaningful, which implies that empty, all-zero, or symbolic attributes are not allowed.
  2. `<rect>`, `<ellipse>`, `<path>` are the only legal svg tag, and the inner `<rect>` must be within the outer `<svg>`.
  3. The id of each tag must be unique and picked from {}.
  4. The position of each tag should be clustered neatly in available areas while avoiding intersection. If intersected, the tags should be resized or moved.

Final: This svg uses canvas\_0 of size (513, 513) with available areas (71, 19, 415, 456) to allocate { text-curved\_1 }.

Figure B. Examples of prompts  $P$  on (a) PKU PosterLayout and (b) PStylish7 datasets.

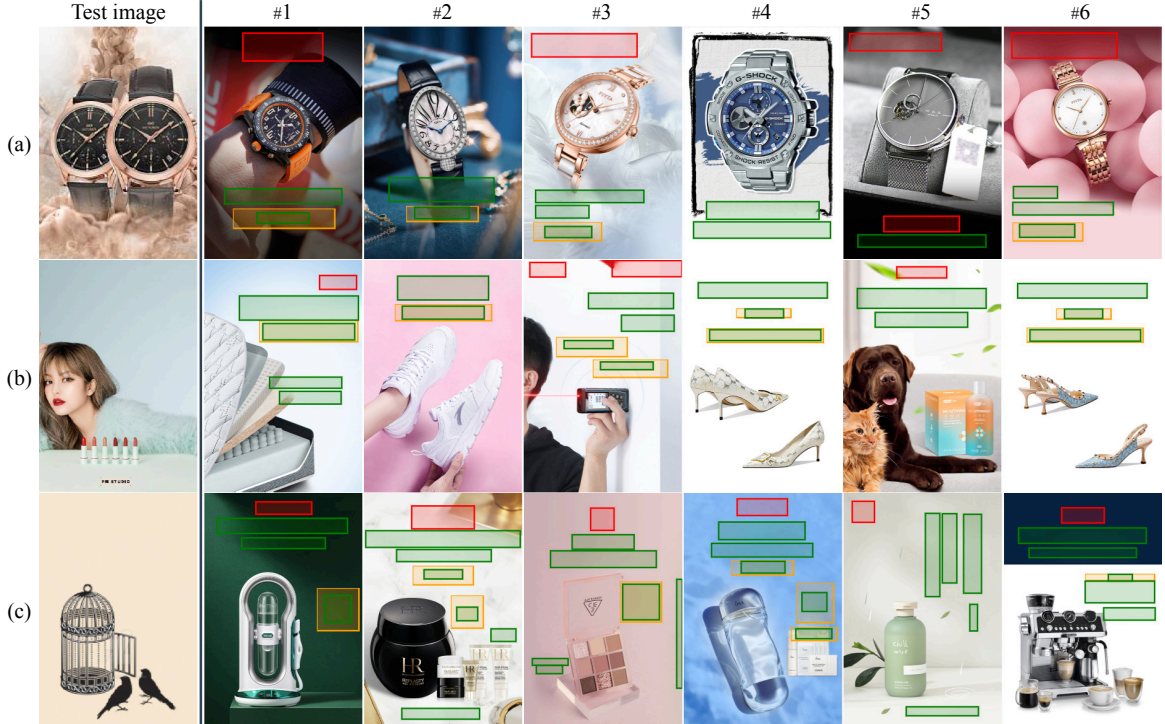


Figure C. Intent-aligned example selection results (#\*) on the *unannotated test split* of PKU PosterLayout dataset.

## B. Additional Experimental Results

**Selected in-context examples.** Fig. C shows the  $k$  layout trees  $\{T_j\}_j^k$  selected as in-context examples that align with the intents of the given test images. By observing (a), we see that the design intent latent space  $\mathbf{Z}_D$  effectively models both semantics and spatial distribution of objects within the images. While the composition of the test images appears similar in (b) and (c), the selection results are very different. These findings demonstrate that our selection procedure provides a comprehensive understanding of visual contents and is sensitive to subtle differences.

**More visualized results.** Fig. D and Fig. E visualize the layouts generated by all baselines [4, 17, 19, 21, 31, 44, 55] and the proposed PosterO. Elements violating graphic metrics and content metrics are respectively indicated by blue and yellow arrows. The comparisons with ground truth demonstrate that PosterO most accurately predicts the design intents and actively utilizes the available areas. Besides, it understands the graphic relationship in layouts well and generates non-overlapping, aligned elements.

**More ablation studies on vision processing.** As reported in Tab. A, we investigate more configurations as follows.

(1) Visual condition vectorization: To demonstrate the advantages of design intent over the widely utilized salient regions, the variant ‘Saliency’ as in LayoutPrompter [31] is implemented. It is observed that all content metrics severely drop, surprisingly, even worse than not performing any vi-

	$Und_i \uparrow$	$Und_s \uparrow$	$Int \downarrow$	$Sal \downarrow$	$Rea \downarrow$	$Avg \downarrow$
Ours	<b>0.9856</b>	<b>0.9241</b>	<b>0.1427</b>	0.2131	0.0248	<b>0.0677</b>
Visual condition vectorization (Ours: Design intent)						
Saliency	0.9694	0.9114	1.2470	1.1867	0.0374	0.3702
Visual information perception (Ours: $d+f$ )						
$-d-f$	0.6873	0.5776	1.1941	0.4980	0.0275	0.3512
$+v$	0.8784	0.6092	0.4868	0.4145	0.0270	0.2063
$+v-d$	0.8874	0.7429	0.3142	<b>0.2078</b>	<b>0.0239</b>	0.1311
$+v-d-f$	0.8335	0.6399	0.6432	0.6116	0.0302	0.2591

Table A. More ablation studies on visual condition vectorization and visual information perception. ( $d$ : Design intent vectorization,  $f$ : Intent-aligned example selection,  $v$ : LLaMA-3-LLaVA-NeXT<sup>8</sup>)

sual perception ( $-d-f$ ). This underscores that design intent is an encouraging substitute for the current saliency paradigm.

(2) Visual information perception: To demonstrate our ( $d$ , Sec. 3.1) vectorized conditions and ( $f$ , Sec. 3.2) learning examples have already considered input images very well, three variants are implemented with ( $v$ ) LLaMA-3-LLaVA-NeXT<sup>8</sup>. It is a large multimodal model (LMM) with powerful visual reasoning capabilities based on Llama 3-8B. However,  $v$  only marginally improves  $Sal \downarrow$  and  $Rea \downarrow$  when it replaces  $d$ , and the rest variants obtain poor results. As our detection model (16M) is much smaller than LLaVA-NeXT’s vision head (encoder: 304M, connector: 20M),  $d$  is a proper alternative. In addition, using  $d$  avoids cross-modal differences between visual tokens and geometric layout elements, reflecting on its better graphic performance.

<sup>8</sup><https://huggingface.co/llava-hf/llama3-llava-next-8b-hf>



Figure D. Visualized results on the *annotated test split* of PKU PosterLayout dataset.



Figure E. Visualized results on the *annotated test split* of CGL dataset.



Figure F. Impact of removing  $h$ : hierarchical nodes in Tab. 5.



Figure G. Results of poster design realization.

Ours <sub>L2</sub>	Paint	Poem	Metro	Movie	Menu	Animal	Insta.
Ove ↓	0.0094	0.0068	0.2622	0.0094	0.0063	0.0085	0.0004
Int ↓	0.4159	0.2402	0.6382	0.7213	0.1260	0.3516	0.1408
Sal ↓	3.1897	0.6106	0.5532	0.5806	0.4312	1.6667	0.0590
Avg ↓	1.2050	0.2859	0.4845	0.4371	0.1879	0.6756	0.0668

Table B. More quantitative results on PStylish7 dataset.

**‘Negative’ impact of hierarchical nodes.** As the enclosing structure is equivalent to *nested layouts*, the current design of  $(h, \text{Sec. 3.1.3})$  hierarchical node representation has effectively constrained the solution space. However, by observing the first two rows of Tab. 5, removing  $h$  appears to improve the standardized content metrics,  $Int \downarrow$  and  $Sal \downarrow$ . To determine the primary cause, we analyzed the visualization results and found a significant occurrence of *empty underlays*, as depicted in Fig. F. These invalids improve in  $Cov$  and  $Uti$ , thereby deceptively enhancing the standardized metrics. This finding again highlights the importance of  $h$  in generating layouts with satisfactory integrity.

**Results of poster design realization.** Sec. 3.3 introduces the zero-shot transformation from generated layouts to actual posters. Fig. G shows the results of each step and the final designs. During *mockup creation*, not only the font size and text color are properly predicted, but also the link to the logo image, *i.e.*, `href` attribute, is correctly created with an initial unknown value. For *material synthesis*, all given contents are perfectly placed into the elements of corresponding `id`. We also request LLMs with *style* in simple words, such as *elegant*, and the resultant posters are astonishingly appealing.

**PosterO<sub>L2</sub> on PStylish7.** In the main text, Tab. 8 reported the quantitative results of PosterO<sub>CL</sub> and PosterO<sub>L3</sub> on PStylish7. Here, Tab. B reports those of PosterO<sub>L2</sub>. Surprisingly, it achieves the best overall performance on *Metro*, *Menu*, *Animal*, and especially *Instagram*. By accumulating

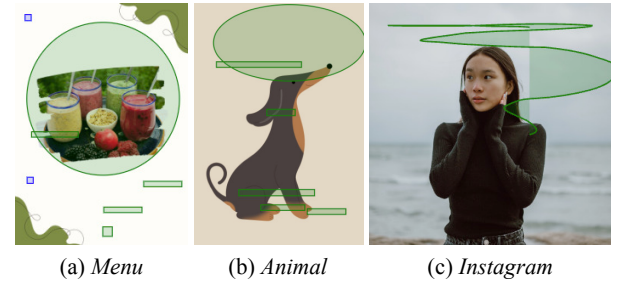


Figure H. Visualized results of PosterO<sub>L2</sub> on PStylish7 dataset.

$Avg \downarrow$  across seven categories, PosterO<sub>L2</sub>, <sub>CL</sub>, and <sub>L3</sub> obtain **3.3427**, 4.3799, and 4.2877, respectively. We visualize some amazing layouts generated by PosterO<sub>L2</sub> in Fig. H.

## C. PStylish7: More Details and Statistics

PStylish7 is the first dataset for generalized content-aware layout generation. We built it with 152 image-layout pairs for few-shot learning and 100 image canvases for benchmark testing. The data comes from a variety of sources, including Canva, Pixabay, Ucshe, and the New York Heritage Digital Collections. In the remaining section, statistics on the distribution of sample categories, element types, and image aspect ratios within the PStylish7 dataset are provided to offer a clear understanding of its diversity and complexity. Additionally, a detailed explanation of the metrics calculation is presented.

### C.1. Statistics

**Sample categories.** The seven categories in PStylish7 are artwork exhibition (*Paint*), cultural education (*Poem*), public safety (*Metro*), entertainment marketing (*Movie*), merchandising display (*Menu*), public advocacy (*Animal*), and social-media interaction (*Instagram*). The distributions of

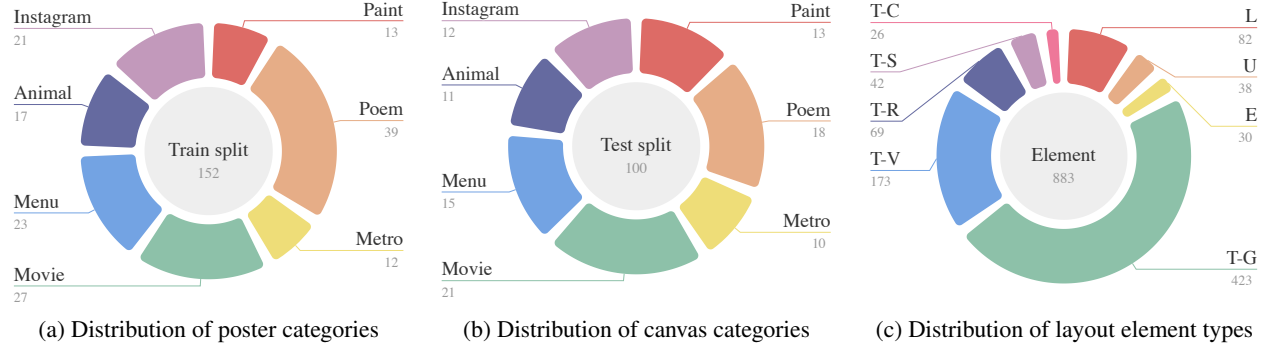


Figure I. Statistics on sample categories and layout element types in PStylish7 dataset.

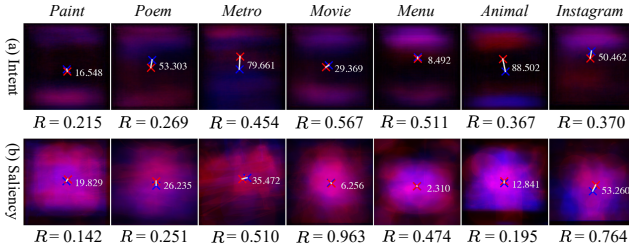


Figure J. Varied difficulty degrees of PStylish7 categories.

samples across different categories in the train and test splits are illustrated in Fig. I(a) and (b).

**Inter-category gaps.** With the diverse purposes and entities in different categories, their difficulty degrees  $H$  are also noticeably varying. To gain insight into  $H$ , we analyzed each category by visualizing the distribution variation  $\Delta D$  between their *train/test* splits and indicating the trade-off factors  $R = \frac{\text{Unmatch}_L}{\text{Match}_L}$  for content metrics, as shown in Fig. J. As observed,  $H \propto \frac{\Delta D}{R}$ , aligning with PosterO’s performance reported in Tab. 8 and Tab. B.

**Layout element types.** The eight layout element types within PStylish7 are logo (L), underlay (U), embellishment (E), and text (T-G, general), along with four text variants (T-V, vertical; T-R, rotated; T-S, ellipse; T-C, complex curve), which are exclusive to this new dataset. The distribution of elements across different types is illustrated in Fig. I(c), showing a total of 883 elements. Notably, over one-third of them are specialized variants, highlighting the dataset’s emphasis on capturing the complexity inherent in real-world design work.

**Image aspect ratios.** The distribution of image aspect ratios within PStylish7 is illustrated in Fig. K. Unlike existing domain-specific datasets [19, 55], where samples are predominantly of a fixed aspect ratio (*i.e.*, 0.68), PStylish7 includes a variety of aspect ratios, with the most common being 5:7 (*i.e.*, 0.71), 9:16 (*i.e.*, 0.56), and 1:1. This highlights the dataset’s emphasis on providing a more realistic conditions for layout generation tasks.

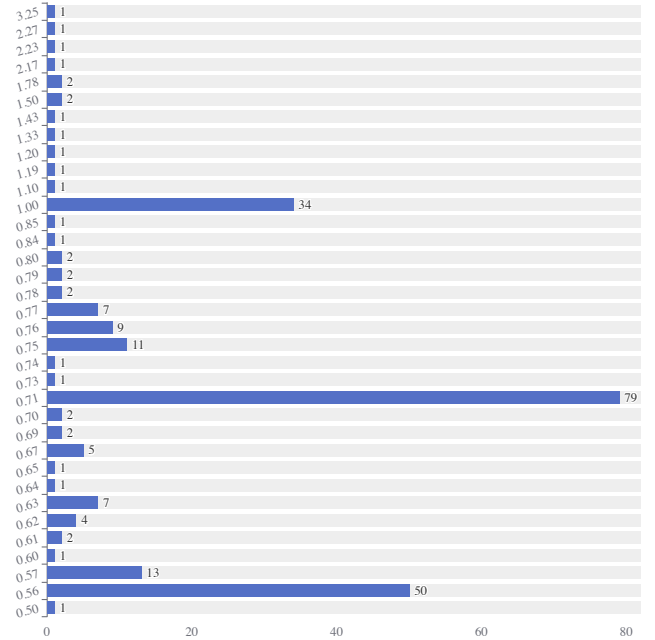


Figure K. Distribution of image aspect ratios in PStylish7 dataset.

## C.2. Metrics

Given the high flexibility of the specialized elements, current numerical metrics (*e.g.*,  $Ali \downarrow$ ) often fail to evaluate their placement and organization. To this end, we resort to pixel-level metrics and regularize the rendering process of element maps for computation. While the content metrics (*i.e.*,  $(Cov \uparrow, Con \downarrow)$ , standardized as  $Int \downarrow$ , and  $(Uti \uparrow, Occ \downarrow)$ , standardized as  $Sal \downarrow$ ) are inherently based on element maps, the graphic ones are not. Therefore, we introduce a pixel-level overlay  $Ove \downarrow$  to fill in this vacancy.

**Element map rendering process.** An element map  $m_{e_i} \in \{0, 1\}^{h \times w}$  serves as the visual indicator revealing the spatial coverage of layout elements  $\{e_i\}_i^n$ . Fig. L illustrates the corresponding element maps of layouts in Fig. H. While rectangular elements are straightforwardly filled with white, those approximated by ellipses and curves require a different way. Concretely, we utilize strokes with a width of 30 pixels to outline these elements. Every element map is uni-

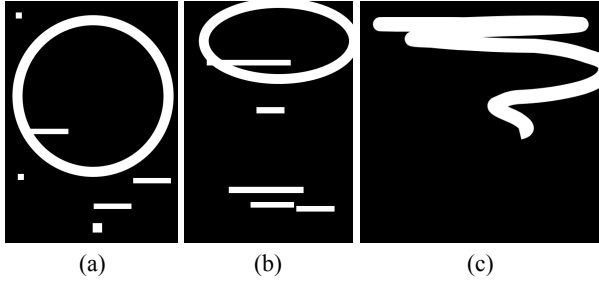


Figure L. Rendered element maps of layouts in Fig. H.

formly scaled to a width  $h$  of 513 pixels to maintain consistency in scale for appropriate comparisons. With our SVG language-based representations, the rendering can be easily implemented by introducing CSS-style declarations as:

```
rect { fill: white; }
ellipse { stroke: white; stroke-width: 30; }
path { stroke: white; stroke-width: 30; }
```

**Pixel-level overlay**  $Ove \downarrow$ . To calculate overlay between non-underlay elements  $\{e_j\}_j^m$ , each element  $e_j$  is rendered individually as a layer  $\ell_j$  of the element map. The overlay is then determined by calculating the sum of layers  $\{\ell_j\}_j^m$  and subtracting the map  $m_{e_j}$  that results from their combination. Specifically, as the maximum value of each pixel in the map is 1, this pixel-level operation accumulates the number of pixels where more than one element is present. By dividing the size of the map  $m_{e_j}$ , we obtain a normalized measure of overlay.